An introduction to Stable Chaos

By:
Matteo Giardi

Supervisors:
Prof. Alessandro Torcini
Prof. Andrea Bacciotti

A thesis presented for the bachelor degree of Matematica per l'Ingegneria.

Dipartimento di Scienze Matematiche
Politecnico di Torino
Date 22-06-17

Abstract

This short bibliographic Bachelor's thesis proposes itself as a first introduction to the study of chaos. In the first part the main tools used in the field are introduced through direct examples and applications: Lyapunov exponents, correlation functions, front propagation, as well as some classical chaotic systems like the logistic and shift maps. In the second part Stable Chaos is presented together with the notion of Chain Map Lattices and some generalization of Lyapunov exponents, comoving and finite size. In the last part, an introduction to Reaction-Diffusion systems is given in order to make a comparison with information propagation in spatially extended chaotic systems.

Contents

Introduction

Edward Lorenz, the father of chaos theory, described chaos in these terms: ”when the present determines the future, but the approximate present does not approximately determine the future”. This is exactly how I got into this subject, almost randomly choosing, among others, a dynamical systems (DS) course for my exchange semester at ETH Zurich. (Although I enjoyed studying this subject very much, I would not have had the chance of further investigation once back at my home university in Turin, had I not decided to make it the core of my Bachelor’s thesis. The idea was to explore a mathematical field and some actual mathematical research in order to see if this could become a possible future career.

This paper will first attempt to put this common but rather mysterious word “chaos” into a mathematical and rigorous framework. When starting with a more classical definition-theorem-proof approach the need to move to a more loose and qualitative approach describing classical examples and modern techniques of investigations becomes immediately clear. However, this should not be seen as a negative aspect but rather the way research on this topic has evolved for years. In the famous paper ”Deterministic Nonperiodic Flow” by Lorenz (1963) one sees much more ”arguments in favour” then real and well-established mathematical proofs. Nonetheless, no one would argue the role of this text in the evolution of the subject.

Secondly, this essay will move to an actual topic of research, that of ”Stable Chaos” (SC), for which very little mathematical theory has been written despite having been investigated extensively via numerical tools for years. I will approach not only its most important characteristics but also the fundamental differences from classical chaotic phenomena- This work will be concluded with a parallel between information propagation in spatially extended systems and front propagation in reaction diffusion systems.

Chapter 1

Deterministic chaos

This first chapter will attempt to give an overview, mainly through direct example, of what deterministic chaos (DS) means and how it could be described, using first formal then more computational tools.

1.1 Chaos: mathematical overview

In this first section we introduce the notion of chaos, and give a key example of a chaotic iterated map, the logistic map, which was popularized in a seminal 1976 paper by the biologist Robert May [10] , in part as a discrete-time demographic model analogous to the logistic equation firstly introduced by Pierre François Verhulst. It should be immediately remarked that there exists no universally accepted definition and we will stick on that given by Devaney R. in [1].

1.1.1 Preliminary definitions

We will initially consider a topological approach to chaos to move later on to a measure theoretic set-up introducing the concept of Lyapunov exponents. As dynamical systems we will consider, whenever differently stated, iterated maps of metric spaces to themselves.

Definition 1.1.1. (Topological transitivity) Let f be a dynamical system on a metric space (X, d). We say f is *topologically transitive* if for any non-empty open subsets U, V of X exists $n \in \mathbb{N}$ such that:

$$f^n(U) \cap V \neq \emptyset$$

Definition 1.1.2. (SIC) Let f be a dynamical system on a metric space (X, d). We say f has *sensitive dependence on initial conditions* (SIC) if there is $\delta > 0$ such that for every $x \in X$ and $\epsilon > 0$ there exist $y \in X$ and $n \in \mathbb{N}$ for which:

$$d(x, y) < \epsilon \Rightarrow d(f^n(x), f^n(y)) > \delta \tag{1.1}$$

What this actually says is that minor changes in the initial state lead to dramatically different long-term behaviours.

Definition 1.1.3. (Chaos) Let f be a dynamical system on a metric space (X, d) with no isolated points. We say f is *chaotic* if:

- f has sensitive dependence on initial conditions.
- f is topologically transitive.
- The set of periodic points of f is dense in X.

Remark 1.1.1. It is possible to show that a dense set of periodic points along with topological transitivity in a space X with isolated points, forces X to be finite and equal to the orbit of one (thus all) of its points.

Definition 1.1.4. (Topological Conjugacy) Suppose $f : X \to X$,$g : Y \to Y$ are dynamical systems. We say that f and g are *conjugate* it there exists a homeomorphism $\phi : Y \to X$ such that the following graph commutes, namely $f \circ \phi = \phi \circ g$:

$$\begin{array}{ccc} Y & \xrightarrow{g} & Y \\ {\scriptstyle\Phi}\downarrow & & \downarrow{\scriptstyle\Phi} \\ X & \xrightarrow{f} & X \end{array}$$

In the following we will consider as proved facts the following topological invariants, i.e. properties that when verified for g are then also true for f, for f and g as before:

- Dense set of periodic points.
- Topological transitivity.

One would actually really like to have chaoticity as a topological property, this theorem comes very handy because frees chaos from being linked to the chosen metric (which defines SIC) thus becoming a topological invariant.

Proposition 1.1.1. Let (X,d) be a metric space without isolated points, $f : X \to X$ a dynamical system, which is both topologically transitive and has a dense set of periodic points. Then f ha SIC w.r.t. any metric defining the topology on X.

One of the first proofs of this appeared on [12], and we omit it.

1.1.2 A recall on 1D stability theory

We first recall some stability properties of iterated maps $f : I \subseteq \mathbb{R} \to \mathbb{R}$:

Definition 1.1.5. (Hyperbolic Point) Let p be a periodic point of minimal period n, then p is *hyperbolic* if $|D(f^n)(p)| \neq 1$, we call this quantity its multiplier.

Proposition 1.1.2. (Attracting Hyperbolic Point) Let p be a periodic point with multiplier less than one and minimal period k, then there exists U open neighborhood of p s.t. $\forall x \in U$:

$$\lim_{n\to\infty} f^{nk}(x) = p$$

We then say p is *attracting* and call U an attracting neighbourhood of p.

Proposition 1.1.3. (Repelling Hyperbolic Point) Let p be a periodic point with multiplier bigger than one, then there exists U open neighbourhood of p and $k \in \mathbb{N}$ s.t. $\forall x \in U, x \neq p, n \geq k$:

$$f^n(x) \notin U$$

We then say p is *repelling* and call U a repelling neighbourhood of p.

Definition 1.1.6. (Hyperbolic Set 1D) A set $\Gamma \subset \mathbb{R}$ is a repelling (resp. attracting) hyperbolic set for f if Γ is closed, bounded and invariant under f and there exists an $N > 0$ such that $|(f^n)'(x)| > 1$ (resp. < 1) $\forall n > N$ and $\forall x \in \Gamma$.

We will then say that a dynamical system is uniformly hyperbolic if the entire space is an hyperbolic set, this idea could be generalized in higher dimensions for diffeomorfisms on manifolds as the splitting of the tangent space in strongly contracting and strongly expanding directions, called stable and unstable manifolds.

1.2 The logistic map

We define the logistic map to be:

$$L_r: \; x_{n+1} = rx_n(1-x_n) \; x \in [0,1] \; r \in [0,4] \tag{1.2}$$

which is a smooth, unimodal i.e. with a unique maximum, continuous, one parameter, map of the unit interval.

As pointed out by Robert May [10], despite appearing very "simple" its dynamic is utterly complicated. In 1976 he introduced this discrete dynamical system as a demographic model, in particular the time n should represent different generations while x_n, ranging in $[0,1]$ was thought to be the ratio of existing population to the maximum possible population. This map could be seen as the discrete version of the continuous system, studied by Pierre Francois Verhulst in 1838:

$$\frac{dN}{dt} = rN - \alpha N^2$$

where $N(t)$ represents the number of individuals at time t, r the intrinsic growth rate, and α is a parameter related to crowding effects.

1.2.1 Emergence of chaos: Non-chaotic regime $r < r_\infty$

We first introduce a new concept:

Definition 1.2.1. A *bifurcation* of a dynamical system f_μ is a qualitative change in its dynamics produced by continuously varying some control parameter μ, namely there exists some value $\mu = \mu_*$ for which the families of C^0 equivalent systems (homeomorphic if f^{-1} invertible) $F_1 = \{f_\mu : \mu < \mu_*\}$ and $F_2 = \{f_\mu : \mu > \mu_*\}$ are not C^0 equivalent to each other i.e. it is not possible to construct a continuous map Φ (homeomorphism if f^{-1} invertible) from a member of F_1 to a member of F_2 and vice-versa.

A *period-doubling bifurcation* corresponds to the creation or destruction of a stable periodic orbit with the period double of the original orbit.

Remark 1.2.1. It is interesting to note that for maps $f : I \subseteq \mathbb{R} \to \mathbb{R}$ as already pointed out we can characterize the attracting behaviour of a n-periodic point by the absolute value of the derivative of f^n, being less then one, this shows that when a stable periodic orbit becomes unstable two possibilities are allowed, namely $Df_\mu^n > 1$ or $Df_\mu^n < -1$. This fact is proper of iterated maps and absent in continuous dynamical systems.

In the case of the logistic map this parameter is r. It has been shown by May (1976), that the dynamic of the logistic map for low values of r follows a so called "cascade of period-doubling bifurcations". There exists in fact a converging increasing sequence $\{\, r_k \mid r_k \in [0,4]\}_{k\geq 0}$ such that for any value of $r_k < r < r_{k+1}$ and for almost all initial conditions x_0, after an initial transient, the trajectory converges to a 2^k-periodic orbit. This fact is made clear in the bifurcation diagram 1.1, in which orbits after their transient behaviour are displayed as a function of $a = r$.

Remark 1.2.2. In the limit r_∞ the attracting orbit becomes infinite and all other (previously attracting) periodic points will have formed a Cantor type, repelling hyperbolic set. A numerical estimation of this value has been found:

$$r_\infty \approx 3.56995$$

We now examine the behaviour of the logistic map for $r_k = 0, 1, 2$:

- $r < r_0 = 1$

  $x^* = L_r(x^*) \Rightarrow x_1^* = 0 \; |\frac{dL_r}{dx}(x^*)| = |r(1-2x^*)| < 1$ thus 0 is an attracting point (population dies out).

- $r_0 < r < r_1 = 3$

  $x^* = L_r(x^*) \Rightarrow x_1^* = 0 \; x_2^* = 1 - 1/r \; |\frac{dL_r}{dx}(x_1^*)| > 1 \; |\frac{dL_r}{dx}(x_2^*)| < 1$ thus $1-1/r$ is an attracting fixed point (population stabilizes to a fixed value).

- $r_1 < r < r_2 = 3.448...$

  $|\frac{dL_r}{dx}(x_1^*)| > 1 \; |\frac{dL_r}{dx}(x_2^*)| > 1$ attracting point x_2^* has become repelling and out of it a stable 2-periodic orbit (fixed point for L_r^2) is born.

Indeed, $x^* = L_r^2(x^*)$ gives 2 new (in addition to x_1^* x_2^*) fixed points $x_{3,4}^* = \frac{(r+1)\pm\sqrt{(r+1)(r-3)}}{2r}$ which are attracting: $|\frac{dL_r^2}{dx}(x_{3,4}^*)| = |\frac{dL_r}{dx}(x_{4,3}^*)\frac{dL_r}{dx}(x_{3,4}^*)| < 1$ (indexes exchange since $L_r(x_{3,4}^*) = x_{4,3}^*$).

- $r_2 < r < ... < r_\infty$

  In the same way, new orbits with periods double than the previous one emerge at the biurcation points.

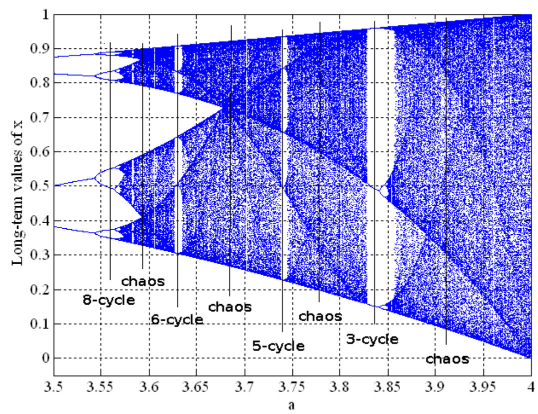

Figure 1.1: Bifurcation diagram for the logistic map, which shows some of the chaotic and periodic windows. This figure is taken from [24].

Remark 1.2.3. for r exactly equal to 3, $x_3^* = x_4^* = x_2^*$ one has $|\frac{dL_r^2}{dx}(x_{2,3}^*)| = 1$ i.e. L_r^2 is tangent to the first quadrant secant at x_2^*. This completes the description of how the doubling described before actually happens(recall that intersections with the secant imply fixed points of the map), one first has, a single real and 2 imaginary solutions ($r < 3$) then 3 real coincident ($r = 3$) and finally 3 real solutions of which 2 form a stable periodic orbit ($r > 3$), where by solution we mean, solution of the system of equations $y = x$, $y = L_r^2(x)$, As in Figure 1.2.

This process increases the complexity and eventually, as we will prove later, leads to chaos. Although this phenomenology might appear a very specific feature of the logistic map, it is proper of the large class of one parameter *smooth unimodal interval maps*, for which some conjectures (Feigenbaum), generalizing their behavior, have been made (Renormalization Theory). As an example, concerning distances (in parameter space) of two consecutive branching a universal constant independent of the studied problem, has been found:

$$\frac{r_n - r_{n-1}}{r_{n+1} - r_n} \to \delta = 4.6692$$

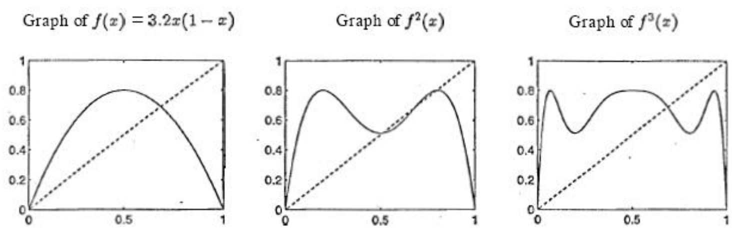

Figure 1.2: Birth of a new periodic orbit. The dashed line being the diagonal of the first quadrant represents all the fixed point of the map. The three images show how a fixed point for L_r^2 i.e. a 2-periodic orbit, has born from one fixed point of L_r and thus also of L_r^3, as described in the text.

1.2.2 Emergence of chaos: Typical chaos $r_\infty < r < 4$

We now qualitatively address the question of what happens for $r_\infty < r < 4$. Looking at the figure 1.1 one can spot "windows", which open with a marked p-periodic behaviour for a certain value r_{p*} and close with chaotic, i.e. completely filled vertical segments (the chaotic attractor is a subset of the unit interval). The most evident is the "period-3 window" marked as "3-cycle" in the figure. What happens is that at $r = 4$, and we will prove this fact rigorously, the chaotic attractor fills the entire unit interval, going backward up to a value r_0' (marked as chaos in the figure immediately before 5-cycle), we have windows ending up in a single smaller and smaller chaotic band, which splits in 2 parts at r_0'. Still proceeding backward one then sees that those chaotic segments get divided more and more to become the infinite-period orbit at r_∞.

It has been shown that those "periodic behaviour windows are dense, however Jacobson found that the probability of randomly choosing a chaotic value of r (eg. r_0') is non-zero and therefore we refer to chaos in the interval $r_\infty < r < 4$ as "typical chaos":

"Each period p window essentially contains a replication of the bifurcation diagram for the map over its whole range. Thus, the windows themselves have windows, which themselves have windows ..." [13] pag. 40.

Remark 1.2.4. What we have seen could be proven using the so called Kneading Theory, a refined version of symbolic dynamic for the specific case of uni-modal maps of the interval.

1.2.3 Special value: r=4

Proposition 1.2.1. The logistic map is chaotic on $I = [0, 1]$ for $r = 4$.

Proof. We will make use of the concept of topological conjugacy and the fact that chaos is a topological invariant, consider the piecewise monotone maps:

$$\text{Define } T\colon [0\ 1] \longrightarrow [0\ 1] \text{ by} f(x) = \begin{cases} 2x & \text{if } 0 \leq x \leq 1/2, \\ 2(1-x) & \text{if } 1/2 \leq x \leq 1. \end{cases} \tag{1.3}$$

$$\text{Define } D\colon [0\ 1] \longrightarrow [0\ 1] \text{ by} f(n) = \begin{cases} 2x & \text{if } 0 \leq x \leq 1/2, \\ 2x - 1 & \text{if } 1/2 \leq x \leq 1. \end{cases} \tag{1.4}$$

Define the homeomorphism, $\phi(x) = sin^2(2x/\pi)$ since $L_4 \circ \phi = \phi \circ T$, then ϕ is a conjugacy from T to L_r.

We see that $T \circ D = T \circ T$ thus $T \circ D^n = T^{n+1}$.

Claim 1.2.1. Let $p \in (0, 1)$. Then p is periodic under T if and only if p is a rational number with even numerator and odd denominator.

Proof. Pick such a p then there will be a positive integer $n \in \mathbb{N}$ such that $D^n(p/2) = p/2$, now $T^n(p) = T^{n+1}(p/2) = T(D^n(p/2)) = T(p/2) = p$ as desired, we will leave the proof of the converse since we won't need it. □

Since such rational numbers are dense in $(0, 1)$ one has also that T has a dense set of periodic points.

Claim 1.2.2. T is topologically transitive.

Proof. It is sufficient to note that $T^k(2m/2^k) = 0$ and $T^k((2m - 1)/2^k) = 1$, pick then $U \subset [0, 1]$ open non-empty, and $m, k \in \mathbb{N}$ sufficiently large that $I = [m/2^k, (m + 1)/2^k] \subset U$ then $T^k(I) = [0, 1]$ which shows $T^k(U) \cap V \neq \emptyset$ for some $k \in \mathbb{N}$. □

Thanks to the conjugacy one has that L_4 chaotic.

□

1.3 Chaos: experimental overview

In this section we will look at some experimental facts about chaos, meaning some aspects, which may not be sufficient nor necessary conditions from a strict mathematical point for chaotic behavior but are useful indicators, mostly being numerically computable quantities.

1.3.1 Lyapunov exponents

We move now to a different point of view of chaos that of ergodic theory, in which we need a measure space equipped with an f-invariant measure, loosely speaking the two approaches are equivalent as soon as one considers a measure which is positive on open sets.

Definition 1.3.1. Lyapunov Exponent Let $f : R^d \to R^d$ be a differentiable map on an open subset $U \subset \mathbb{R}$ into itself, and let

$$D(f^n)(x) \circ v$$

denote the derivative of f^n at x in the direction v. For $x \in U$ define the *Lyapunov Exponent* (LE), $\lambda(x, v)$ by:

$$\lambda(x, v) = \limsup_{n\to\infty} \frac{1}{n} \ln \|D(f^n)(x) \circ v\| \tag{1.5}$$

The LE is then a measure of the exponential growth rate of tangent vectors along orbits [2], indeed if f has uniformly bounded derivative LE is well defined. Considering an orthonormal base for our space one could therefore calculate an entire "spectrum" of exponents.

There is a strong connection between positivity of Lyapunov exponents and SIC, indeed one has for $\lambda(x,v) > 0$ a sequence $n_j \to \infty$ such that:

$$\|Df^{n_j}(x) \circ v\| \geq e^{(\lambda(x)-\epsilon)n_j}\|v\| \text{ with } \ \epsilon > 0$$

Which shows the existence of $y \in U$ such that for any $\epsilon > 0$:

$$d(f_j^n(x), f_j^n(y)) \geq \frac{1}{2}e^{(\lambda(x)-\epsilon)n_j}d(x,y)$$

Now the distance from x,y is not arbitrary small as required to have SIC, thus considering the topological definition given, positive Lyapunov exponents do not imply dependence on initial conditions. However one has:

Proposition 1.3.1. Sensitive dependence on initial conditions implies that for some point x there exists a direction v such that the associated Lyapunov exponent is positive.

Proof. Thanks to the Mean Value Theorem if say y, z arbitrarily closed points are moved far apart after n application of f then there must be another point x and a direction v for which$\|Df^{n_j}(x) \circ v\| > \|v\|$, as wished. □

We recall here some result which will clarify the relation between chaos and positive Lyapunov exponents, for simplicity we will assume a 1D system (thus only one possible direction v), but those arguments suitable reformed hold also in higher dimensions [14]:

The chain rule for an initial condition x_0 and $x_i = f^i(x_0)$, gives:

$$Df^n(x_0) = Df(x_n)Df^{n-1}(x_{n-1}) = \prod_{i=0}^{n-1} Df(x_i)$$

Now assuming the existence of an ergodic measure μ for f, Birkhoff's Ergodic Theorem [2], gives:

$$\lambda(x_0) = \limsup_{n\to\infty} \frac{1}{n} \log \mid Df^n(x) \mid = \limsup_{n\to\infty} \frac{1}{n} \sum_{i=0}^{i=n-1} \log \mid Df(f^i(x_0)) \mid = \int_X \log \mid Df(f^i(x)) \mid d\mu$$

thus $\lambda(x_0) = \lambda$ for almost all $x_0 \in X$.

Now if one considers $d(x,y) = \delta x_0$ as a perturbation of the initial state x_0, then neglecting higher order terms in the Fourier expansion:

$$\delta x_n = d(f^n(x), f^n(y)) = d(f^n(x_0+\delta x_0), f^n(x_0)) \approx |f^n(x_0)+Df^n(x_0)\delta x_0 - f^n(x_0)| = |Df^n(x_0)|\delta x_0$$

We could then regard Lyapunov exponents as the rate of information created by the system with time i.e. complexity and chaoticity.

$$\delta x_n \sim e^{\lambda n}\delta x_0 \tag{1.6}$$

A new definition of chaos could then be considered [15]:

Definition 1.3.2. (Observable Chaos) We say that f has *observable chaos* if $\lambda_{MAX} > 0$ on at least one positive Lebesgue measure set A, where λ_{MAX} represents the maximum Lyapunov exponent at some $x \in A$.

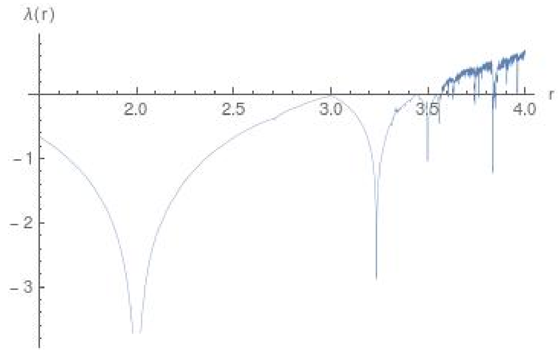

Figure 1.3: Maximum Lyapunov exponent as a function of the parameter r, for the Logistic map, the figure clearly shows a general increasing trend toward positive values i.e. chaotic behaviour, mixed with very negative peaks, confirming the existence of stable periodic windows.

1.3.2 Strange Attractors

In dissipative systems i.e. systems where the volume in the phase space contracts with time, are usually characterized by special type of attractors i.e. sets on which trajectories settle after an initial thus transient behaviour. In fact those systems are very common in physical applications, consider as an example the famous Lorenz system which was initially proposed as a mathematical model of atmospheric convections, it has been shown to have exponential volume contraction which leads to the creation of the so called Lorenz Attractor [19].

"Such objects often arise when a diffeomorphism f stretches and folds an open set U and maps the closure $f(\bar{U})$ inside U (this is a typical situation, not a necessary or a sufficient condition). The strange attractor A is visualized when a computer plots the points $x_n = f^n(x_0)$ with almost any initial value x_0 in U." [3]

Although there is no universally accepted definition Ruelle [4] defines it to be an *uniformly hyperbolic attractor*:

Definition 1.3.3. (Uniformly Hyperbolic Attractor) A bounded set A is said to be a *uniformly hyperbolic attractor* for a dynamical system f if it is an hyperbolic set and there exist an open non-empty neighborhood of A such that:

1. $\bigcap_{n\geq 0} f^n(U) = A$.
2. Points in U have SIC.

3. There is no proper subset of A for which (1) and (2) hold.

Condition one express the fact that A is attracting, while condition two makes evident the fact that is strange, finally condition three makes it indecomposable.

"There are points y close to $x \in A$ such that the distance between $f^n(x)$ and $f^n(y)$ grows exponentially with n until this distance becomes of the order of the diameter of A. The exponential growth of $\text{dist}(f^n(x), f^n(y))$ expresses chaos, or sensitivity to initial condition: if there is any imprecision on x, the predictability of $f^n(x)$ is lost for large n. Here, f stretches the set U and necessarily also "folds" this set to put $f(\bar{U})$ back in U." [3]

As cleared by Pesin in [20], the study of uniform hyperbolicity is of great mathematical interest but has little physical relevance, generalisations of this concept as non uniform hyperbolicity and partial hyperbolicity "allows for great applications outside of mathematics, such as to physics, biology, engineering, and so on."

Hyperbolic sets and the logistic map

In this section we show the existence of a chaotic hyperbolic set for $r > 2 + \sqrt{5}$. We will make use of symbolic dynamics which will prove to be a very powerful tool in this context.

Definition 1.3.4. Let $\sum_2^+$ denote the space of infinite binary sequences $\mathbf{x} = (x_0, x_1, ...)$ $x_k \in 0, 1$ equipped with the metric d:

$$d(\mathbf{x}, \mathbf{y}) = \sum_{k=0}^{\infty} \frac{|x_k - y_k|}{2^k}$$

Moreover let the shift map $\sigma : \sum_2^+ \to \sum_2^+$ be:

$$\sigma(x_0, x_1, ...) = (x_1, x_2, ...)$$

We will assume the following facts about σ and $\sum_2^+$:

- $\sum_2^+$ is homeomorphic to the cantor set.
- σ is a chaotic continuous map.

Symbolic dynamics

The main idea of symbolic dynamic is to partition the space (or a subset we want to focus on) in, say n subsets and to each one attribute a symbol. Orbits could then be regarded as infinite sequences of formal symbols i.e. elements of $\sum_n^+$,the evolution in time gives itineraries between different sets and is then resembled by the shift operator σ. This clearly creates an "uncertainty" given by the max of the diameters of all the subsets.

Since we have $r > 4$ the whole unit interval I is no more forward invariant thus we will restrict the domain of L_r to a new invariant subset $\Lambda \subset I$. In our case the so called Markov Partition will be:

Proposition 1.3.2. Define inductively:

$$A_0 = \{x \in I | L_r(x) \notin I\} \Rightarrow A_i = \{x \in I | L_r(x) \in A_{i-1}\}$$

Then $\Lambda = I - \bigcup_i A_i$ is a Cantor set for $r > 2 + \sqrt{5}$, and is made of all those points in I that under positive iterates of L_r don't leave I.

Proof. Define $I_0 = [0, x_-], I_1 = [x_+, 1]$with$x_\pm = \frac{1 \pm \sqrt{1-4/r}}{2}$ Looking at the graph 1.4 one sees that $L_r(I_0) = L_r(I_1) = I$ thus there must be two open intervals in I_0 and I_1 mapped in A_0 thus escaping I after two iterations so that one has four closed intervals $I_{00}, I_{01}, I_{10}, I_1$ whose points are mapped outside I after two iterations, this inductively, gives a nested sequence of non-empty closed intervals, the limit, thanks to Cantor's Intersection Theorem, exists, and is a closed non-empty set as well and is by definition Λ, i.e. the set of points not leaving I after infinite iterations.

We first need a lemma:

Lemma 1.3.1. If $r > 2 + \sqrt{5}$ then $|D(L_r)(x)| > 1 \ \forall x \in \Lambda$

This combined with the subsequent results shows that Λ is Hyperbolic.

Proof. $|D(L_r)(x)| = |r(1-2x)| > 1$ pick $x = x_+$ then one has $\sqrt{r^2 - 4r} > 1 \Rightarrow r > 2 + \sqrt{5}$ □

We have to show that Λ is perfect and totally disconnected:

- **Perfect**: The construction shows that is closed, suppose now x is an isolated point of Λ then there would be an open neighbourhood U of x s.t. $U - \{x\} \cap \Lambda = \emptyset$ which implies that all points of U except for x are mapped outside I i.e. they belong to A_k for some k. We distinguish two cases:

  1. There is a sequence of A_k whose endpoints converge to x.
  2. Nearby points are mapped outside I by the same iteration of L_r.

  To rule out the first case is sufficient to note that those points are all mapped to $0 \in \Lambda$ after some iteration (look at the graph and use induction), and thus belong themselves to Λ, preventing x from being isolated. In the latter case x is the endpoint of some A_k and thus we may assume is mapped to zero while its neighbors are mapped outside I, but this is possible only if x is a maximum i.e. using the chain rule: $D(L_r^k)(x) = \prod_{i=1}^k D(L_r)(L_r^i(x)) = 0 \Leftrightarrow \exists\ i \leq k$s.t. $D(L_r)(L_r^i(x)) = 0 \Leftrightarrow L_r^i(x) = 1/2$ but then $L_r^{i+1}(x) \notin I$ which is absurd since we where assuming $L_r^i(x) \to 0$.

- **Totally disconnected**: Suppose exists $[x, y] \subset \Lambda$ the lemma gives $|D(L_r)(x)| > \lambda > 1$ implying $|L_r^j(x) - L_r^j(y)| > \lambda^j |x - y| > 1$ but then one would have either $L_r^j(x)$ or $L_r^j(x)$ not in Λ which is absurd since $x, y \in \Lambda$ by assumption. So we have proved there no closed intervals are contained in Λ, i.e. is totally disconnected.

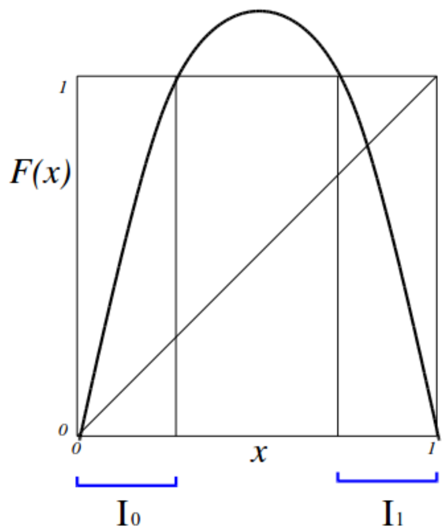

Figure 1.4: Markov Partition described in the text. One clearly sees that point which not lie in I_0, I_1 are sent from $F(x) = L_r(x)$ outside the interval.

□

Remark 1.3.1. It is possible to show that Λ is a repelling Hyperbolic Cantor set for $r > 4$ using a refined version of Symbolic Dynamics which is based on shifts of finite type i.e. with a restricted domain of the shift map to the L_r-admissible sequences only. Moreover, one can show that for $r = r_\infty$ a different hyperbolic Cantor set exists as well. Unfortunately in both cases the finite shift operator is not chaotic (in a topological sense).

Proposition 1.3.3. If $r > 2 + \sqrt{5}$ then $S : \Lambda \to \sum_2^+$ is a homeomorphism. Where S is the itinerary map defined by:

$$S(x) = (s_0, s_1, ...) \text{ with } s_j = \begin{cases} 1 & \text{if } L_r^j(x) \in I_1, \\ 0 & \text{if } L_r^j(x) \in I_0. \end{cases}$$

Proof. **Injectivity:** Suppose there exists $x, y \in \Lambda$ with $x \neq y$ and $S(x) = S(y) = \mathbf{s}$. Then (from the definition of $\mathbf{s}$) we see that $L_r^j(x)$ and $L_r^j(y)$ are always on the same side of $p = 1/2$ (since they are always in the same interval I_0 or I_1) which is $|L_r^j(x) - L_r^j(y)| < 1/2 \ \forall \ j \geq 1$. The lemma ensures that $|D(L_r)(x)| > \lambda > 1$ implying $|L_r^j(x) - L_r^j(y)| > \lambda^j |x - y| \ \forall \ j \geq 1$, thanks to the Mean Value Theorem. One then has that the right-hand side eventually becomes greater than 1/2, so there is a contradiction unless $|x - y| = 0$ which means we must have $x = y$.

Surjectivity: Given an itinerary $\mathbf{s} = (s_0, s_1, ...)$ we need to show there exists $x \in \Lambda$ such that $S(x) = \mathbf{s}$. We first note that $I \cap L_r^{-1}(I) = I_0 \cup I_1$, define inductively the refinement of of our partition to be:

$$I^n = I_{s_0} \cap L_r^{-1}(I_{s_1}) \cap ... \cap L_r^{-n}(I_{s_n})$$

This procedure allow us to locate better, as n increases, the initial condition i.e the position x which is represented symbolically by $\mathbf{s}$ since if $x \in I^n$ then $L_r^i(x) \in I_{s_i}$ for $1 \leq i \leq n$.

We now claim that I^n is a nested sequence of non-empty closed intervals thus by Cantor's Intersection Theorem I^∞, limit of the sequence is non-empty as well, proving the existence of an x represented by $\mathbf{s}$ which will then be unique thanks to injectivity.

Arguing as in the proof above one shows that $I^1 = I_{s_0} \cap L_r^{-1}(I_{s_1})$ is a non empty closed subset of I_{s_0} what ever s_0,s_1, by induction on n one then has I^{n-1} is closed and nested as well. Moreover:

$$I^n = I_{s_0} \cap L_r^{-1}(I^{n-1})$$

is closed being a finite intersection of closed sets, non-empty and nested since, inductively one has $I^{n-1} \subset I_0$, and by definition $I^n = I^{n-1} \cap L_r^{-n}(I_n) \subset I^{n-1}$ this proves the induction step and therefore the claim.

Continuity of S, S^{-1}: Set $\mathbf{s} = (s_1, s_2, ...) = S(x)$, $\mathbf{t} = (t_1, t_2, ...) = S(y)$ now the following double implications follow: $x \to y \Leftrightarrow$ for some sequence j_k $|L_r^{j_k}(x) - L_r^{j_k}(y)| < 1/2 \Leftrightarrow s_{j_k} = t_{j_k} \Leftrightarrow d(\mathbf{s}, \mathbf{t}) \to 0$. □

This theorem fabricates a conjugacy between the shift operator and the restricted logistic map on Λ for $r > 2 + \sqrt{5}$. Thus the logistic map is chaotic on this new domain and we can classify Λ as being a strange attractor.

Chapter 2

Stable Chaos

In this chapter the main topic is discussed, here we adopted a more computational and qualitative approach to the subject, in order to make immediate and clear, differences and similarities, of this strange phenomenon with respect to the deterministic counterpart. Although appearing as an oxymoron [11], the statement "stable chaos" has nothing contradictory in it. It refers to a special class of systems for which despite being the maximum LE negative (stable), particularly long and unpredictable transients characterize the actual dynamics. The discovery of SC is linked to coupled discontinuous maps, recent studies in the field of neural networks [16] showed the relevance of SC in physical models, as well.

2.1 A brief introduction

In this section the concept of spatially coupled systems is introduced, as this is the environment in which stable chaos will be studied.

2.1.1 CML and Spatio-Temporal Chaos

To observe the phenomenon of SC one has to consider high-dimensional spatially extended chaotic systems, it is, in fact, strongly linked with the concept of spatio-temporal chaos. This phenomenon arises when, considering dynamics at different locations in space for a fixed time t, unpredictability is displayed. In those kind of system one has then, to take into account evolution in space and time to fully characterize chaoticity.

Moreover, SC has mostly been found in a special class of such high-dimensional systems called *coupled map lattices* CML, which are systems:

- **Discrete in space:** the "spaces" in which CML live are networks, as in figure 2.1, important parameters are then the number of sites along with the degree and strength of connections of the lattice itself. In particular

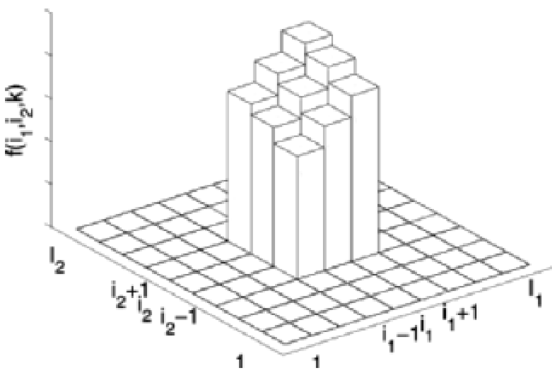

Figure 2.1: CML $f(i_1, i_2, k)$, defined on two coupled sites i_1, i_2, and evolving with discrete time k. This figure is taken from [7].

the so called "thermodynamical limit" i.e. when one consider an infinite number of points, becomes an interesting limit-behavior to be studied.

- **Discrete in time:** we consider at each site in space an iterated map, whose image is affected to some extent, by the behaviours of neighbours, throughout coupling parameters.
- **Continuous state:** the possible range of states occupied by the system varies in a continuous way, despite space and time variables being discrete.

Proved in [21], the existence of invariant measures (counterparts of SRB measures in high dimensionality) guarantees the meaningfulness of studying objects like Lyapunov exponents, in that makes them well defined almost everywhere.

In particular we will consider a 1D model of diffusively coupled maps, of the type:

$$x_i(t+1) = (1-\epsilon)f(x_i(t)) + \frac{\epsilon}{2}[f(x_{i-1}(t)) + f(x_{i+1}(t))] \tag{2.1}$$

with $\epsilon \in [0,1]$ being the coupling strength and f being the piecewise continuous ($\eta > 0$) linear map, defined by:

$$f(x) = \begin{cases} p_1 x + q_1 & \text{if } 0 \le x \le x_c, \\ 1 - (1-q_2)(x-x_c)/\eta & \text{if } x_c < x \le x_c + \eta, \\ q_2 + p_2(x - x_c - \eta) & \text{if } x_c + \eta < x \le 1. \end{cases} \tag{2.2}$$

with $x_c = (1-q_1)/p_1$. This represents a chain of coupled DS (Figure 2.2), in general periodic boundary conditions are chosen, namely if N is the length of the system then $x_{N+1} = x_1$.

2.2 Some new tools

In this section we describe some very general computational tools that have proved to be very useful in the study of SC.

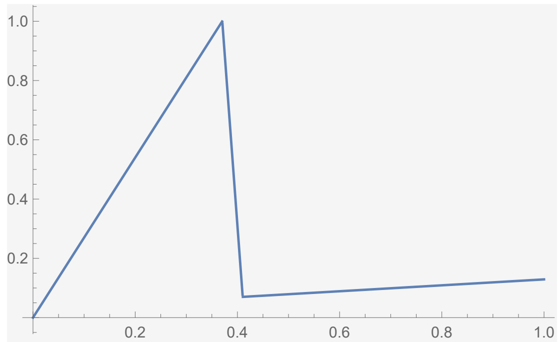

Figure 2.2: $f(x)$, as described in the text with parameters, p1 = 2.7, q1 = 0, q2 = 0.07, p2 = 0.1, η=0.04, except for the value of η the others are the ones considered hereafter unless otherwise stated.

2.2.1 Comoving LEs

In order to study evolution of infinitesimal perturbations on networks one has to consider both spatial and temporal components of the problem. In particular it is useful to adopt a so called chronotopic approach. One should consider generic perturbations with exponential profile in both space and time.

$$|\delta u_i(t)| \propto e^{\lambda t - \mu i} \Rightarrow \begin{cases} \delta u_i(t) = \phi_i(t) \exp(\mu i), \\ v(\mu) = \lambda(\mu)/\mu. \end{cases} \tag{2.3}$$

This leads to the definition of specific or temporal Lyapunov exponents:

$$|\delta u_i(t)| \simeq |\delta u_i(0)| e^{\lambda(\mu) t} \tag{2.4}$$

where μ represents the spatial growth (or decrease) rate of the perturbation. and of spatial Lyapunov exponents:

$$|\delta u_i(t)| \simeq |\delta u_0(t)| e^{\mu(\lambda) i} \tag{2.5}$$

Another approach is that of perturbing the system at the origin and calculate the LEs on a reference frame moving at constant velocity v. One considers perturbations with exponential profile :

$$|\delta u_i(t)| \simeq |\delta u_0(0)| e^{\Lambda(v=i/t)t} \Rightarrow \delta u_i(t) = \phi_i(t) \exp(\mu i) \tag{2.6}$$

Where $\Lambda(v)$ is the largest comoving Lyapunov exponent along the world line $i = [vt]$ (where $[\cdot]$ stands for the integer part operator), whose operative definition is given by:

$$\Lambda(v) = \lim_{t \to \infty} \lim_{L \to \infty} \lim_{|\delta u_0(0)| \to 0} \frac{1}{t} ln \frac{|\delta u_i(t)|}{|\delta u_0(0)|} \tag{2.7}$$

Remark 2.2.1. The function $\Lambda(v)$ has a typically parabolic shape [5] and is such that:

- $\Lambda(v = 0) = \lambda_{max}$ if the moving reference frame is at rest one recovers the standard definition of LE.
- $\Lambda(v_L) = 0$ when the velocity of the moving frame resembles that of the linear perturbation the relative velocity is null i.e. the perturbation neither decreases nor increases. This actually proves to be useful when considering the evolution of infinitesimal perturbations, in that one can, solving the above equation find v_L.

Remark 2.2.2. It will be particularly important for the study of SC to note the order in which limits are taken: the thermodynamical limit should come before looking at the long term behaviour ($t \to \infty$) or otherwise the perturbation would, in a finite time, reach the border of the chain, moreover, in order to consider only linear effects on the perturbation, and therefore avoid possible saturations due to non-linearities, the infinitesimal sized perturbation limit, $|\delta u_0(0)| \to 0$ has to be taken first.

It is possible to calculate the comoving spectrum via linearisation:

$$\mathbf{u}(t+1) = \mathbf{F}(\mathbf{u}(t))$$

This was done in [22] but here for simplicity, we will concentrate on the maximum exponent only. To calculate the latter one should make use of the Legendre transform between specific and comoving LE:

$$(\lambda(\mu), \mu) \leftrightarrow (\Lambda(v), v)$$

which is given by:

$$\lambda(\mu) = \Lambda(v) - v\frac{d\Lambda(v)}{dv} \tag{2.8}$$

Proof. From the definition of specific Lyapunov exponent $\lambda(\mu)$ one has:

One can the consider the expansion for long times:

$$\Lambda(\frac{i+1}{t}) \simeq \Lambda(\frac{i}{t}) + \frac{d\Lambda(v)}{dv}\Delta v$$

with $\Delta v = \frac{i+1}{t} - \frac{i}{t} = \frac{1}{t}$.

One could then find an expression for μ by means of (2.4) and $i = vt$:

$$\frac{|\delta u_{i+1}(t)|}{|\delta u_i(t)|} \simeq \frac{e^{\Lambda(\frac{i+1}{t})t}}{e^{\Lambda(\frac{i}{t})t}} = e^{\frac{d\lambda(v)}{dv}}$$

$$\mu = \ln\frac{|\delta u_{i+1}(t)|}{|\delta u_i(t)|} = \frac{d\Lambda(v)}{dv}$$

which gives exponential growths :

$$|\delta u_i(t)| \simeq |\delta u_0(t)| e^{\mu i} \Rightarrow |\delta u_i(0)| \sim |\delta u_0(0)| e^{\mu i}$$

Substituting in (2.7) and comparing with (2.4):

$$|\delta u_i(t)| \simeq |\delta u_0(0)| e^{\mu i + \lambda(\mu) t} \simeq |\delta u_0(0)| e^{\Lambda(v) t} \Rightarrow \mu i + \lambda(\mu) t = \Lambda(v) t$$

Which is (2.6). The inverse transform reads, then:

$$\frac{d\lambda(\mu)}{d\mu} = -v \tag{2.9}$$

□

Remark 2.2.3. For a numerical routine generally used to find the Lyapunov spectrum see for example [23].

2.2.2 Finite Size LEs

Linear analysis of a system is indeed very useful to predict long-term behaviors but for example when the non-linear part of the dynamics becomes preponderant it won't be as effective. One then has to focus on finite time scales and finite perturbations rather then infinite time and infinitesimal perturbation. It would anyway be desirable to apply linear techniques also in this context, to this end, Finite Size Lyapunov Exponents (FSLEs), were introduced. Since those quantities have a less firm mathematical background [7], an operative definition will be given.

According to the definition of the Lyapunov exponent, for initial uncertainty δ_0, perturbation at time t equal to δ_t, in the limit $|\delta_0| \to 0$, one can write:

$$|\delta_t| \simeq |\delta_0| e^{\lambda t}$$

Which gives a new way of calculating the exponent as:

$$\lambda = \lim_{t\to\infty} \lim_{|\delta_0|\to 0} \frac{1}{t} \ln \frac{|\delta_t|}{|\delta_0|}$$

from this one can extract an effective Lyapunov exponent, for final perturbation δ, over a time T, as:

$$\gamma = \frac{1}{T} \ln\left(\frac{\delta}{\delta_0}\right)$$

The idea is the following, we pick a trajectory on the attractor and perturb it, wait until the perturbation has grown by $\delta_n = \rho^n \delta_0$, (for small w.r.t the size of the attractor δ_0) and calculate the time τ_1 it takes to increase from δ_n to δ_{n+1}, we than we then pick the non perturbed orbit at τ_1, perturb it and wait as done before obtaining a new time interval τ_2, repeat this procedure N times,

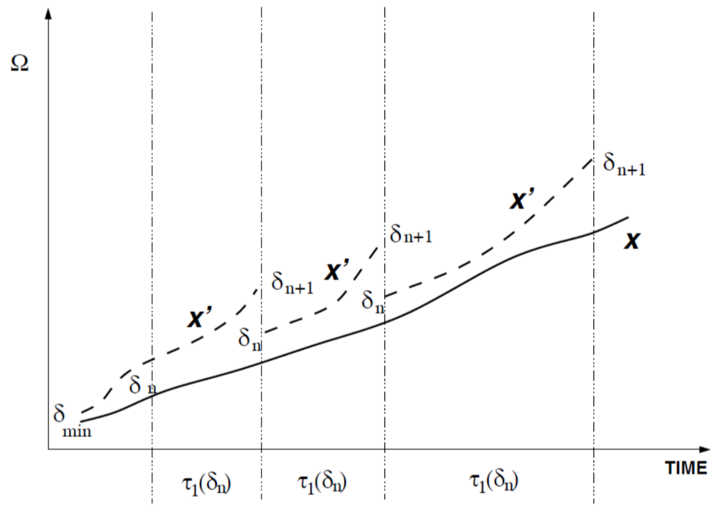

Figure 2.3: Algorithm for computing the FSLE, where one perturbs repeatedly and orbit and waits for a certain increment. This figure is taken from [7].

finally averaging all data, we determine the FSLE as an effective Lyapunov exponent over the length scale δ_n, and time interval $T = \sum_i \tau_i$, for a graphical explanation see figure 2.3.

Due to the fact that our system is discrete in time the above algorithm assumes the following form: we consider a reference trajectory (which should be chosen on the attractor in order to avoid transient effects) at x_0 and a perturbed one $\tilde{x_0} = x_0 + \delta x_0$, with $||\delta x_0|| = \delta_0$, we choose a finite number N of samplings and an interesting scaling factor ρ (usually $1 < \rho \leq 2$), define:

$$\delta(\tau) = \|x_\tau - \tilde{x_\tau}\|$$

$$\delta_n = \rho^n \delta_0$$

Now for $i = 1, ..., N$ we consider time intervals: $\tau_i(\delta_n)$ as the minimum times τ the perturbation takes to increase from δ_n to $\delta(\tau) \geq \delta_{n+1}$ at the i-th iteration of the procedure above, where $\geq$ is due to the discreteness in time.

Calculate:

$$\gamma_i = \frac{1}{\tau_i(\delta_n)} \ln\left(\frac{\delta(\tau_i(\delta_n))}{\delta_n}\right)$$

The FSLE is then given by:

$$\lambda(\delta_n) = \frac{1}{\langle \tau(\delta_n) \rangle} \left\langle \ln\left(\frac{\delta(\tau(\delta_n))}{\delta_n}\right) \right\rangle \Leftarrow \begin{cases} \left\langle \ln\left(\frac{\delta(\tau(\delta_n))}{\delta_n}\right) \right\rangle = \frac{\sum_i \gamma_i \tau_i}{\sum_i \tau_i}, \\ \langle \tau(\delta) \rangle = \sum_i \frac{\tau_i}{N}. \end{cases} \quad (2.10)$$

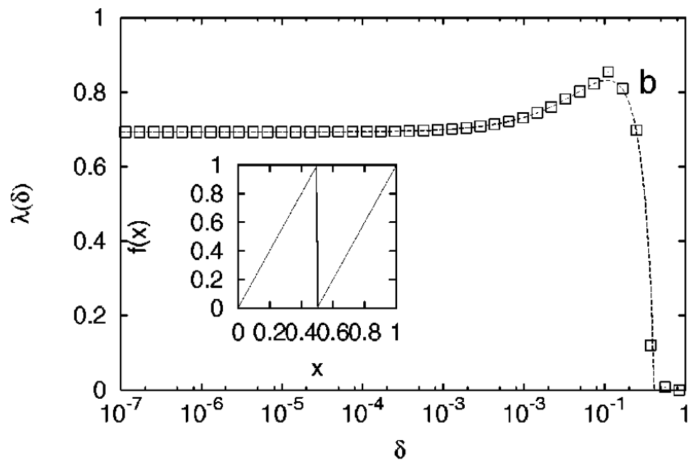

Figure 2.4: $\lambda(\delta)$ versus δ for the Bernoulli shift map. The continuous line is the analytical estimation of the FSLE. The map itself is shown in the inset. One clearly sees that around 0.1 the plateaux which has value $\lambda = \lambda(0)$ i.e. the classical Lyapunov exponent grows making $\lambda(\delta) > \lambda(0)$. This figure is taken from [9].

Remark 2.2.4. The amount of perturbation δ is not completely arbitrary and should be such that $\delta < \langle \|x-y\| \rangle_\mu$, where μ is a natural measure for the system, $\|\cdot\|$ is some chosen norm, and x, y are arbitrary points on the attractor. This fact also makes clear that this tool is intrinsically not well defined since the choice of the norm strongly influences the results.

To make the procedure clearer, and to highlight some properties of discontinuous maps which will be useful later we calculate LE and FSLE for the Bernoulli shift map [9]:

$$f(x) = 2x \bmod 1$$

choose $\tau(\delta) = 1$, then:

$$\lambda(\delta) = \left\langle \ln \left| \frac{f(x+\delta/2) - f(x-\delta/2)}{\delta} \right| \right\rangle = \langle I(x, \delta) \rangle$$

for delta not to large:

$$I(x, \delta) = \begin{cases} \ln[2(2x-1)/\delta] & \text{if } x \in [1/2 - \delta/2, 1/2 + \delta/2], \\ \ln 2 & \text{else} \end{cases}$$ recall that the Lebesgue measure is ergodic for this DS, thus integrating one has:

$$\lambda(\delta) = (1-\delta)\ln\beta + \delta \ln\left(\frac{1-\beta\delta}{\delta}\right)$$

$$\lambda = \lambda(0) = \ln(2)$$

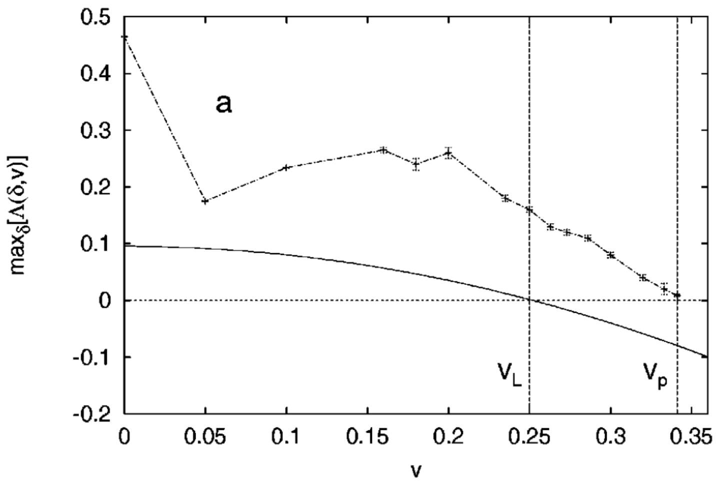

Figure 2.5: linear prediction $\lambda(V_L) = 0$ and finite sized prediction $\max_\delta\{\lambda(\delta, V_p)\} = 0$ of front propagation speeds, for coupled shift maps with parameters $\beta = 1.1$ and $\epsilon = 1/3$. $x_i(t+1) = (1-\epsilon)\beta x_1(t) + \epsilon\beta x_2(t) \mod 1$ $i = 1, 2$. This figure is taken from [9].

This shows that for some values of delta $\lambda(\delta) > \lambda$, this behavior has to be linked with the fact that, when 2 points , near the discontinuity $x = 1/\beta$, are chosen, they will probably move far apart faster the other points as time goes on. This phenomenon in which finite instabilities influence the dynamics has been found also in continuous coupled maps (Figure 2.5) and is key in SC, where evolution is mainly characterized by those. In particular the fact that the FSLE is bigger then the LE is a clear sign of non-linear contributions to the dynamics.

2.2.3 Correlation functions

A way to characterize a signal changing in time $x(t)$ (one could also extend the notion for space), is via its auto-correlation function $C(\tau)$. Assuming the system statistically stationary (time-invariant joint probability distributions) one defines this new quantity to be [7, pag. 62]:

$$C(\tau) = \langle x(t+\tau) - \langle x(t)\rangle)(x(t) - \langle x(t)\rangle)\rangle = \langle x(t+\tau)x(t)\rangle - \langle x(t)\rangle^2 \quad (2.11)$$

$$\langle x(t)\rangle = \lim_{T\to\infty} \frac{1}{T}\sum_{t=0}^{T-1} x_t = \int_\Omega x(t)d\mu$$

where the last equality holds for ergodic systems, with μ a suitable invariant measure, and Ω the phase space. The behavior of $C(\tau)$ gives a first insight of the

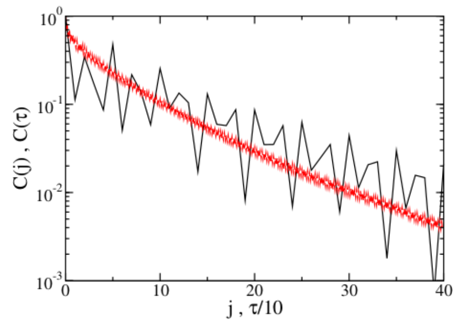

Figure 2.6: Spatial and temporal (smoother curve) correlations for $\epsilon = 0.608$. This figure is taken from [5].

system global behavior, indeed for periodic or quasi-periodic systems $C(\tau)$ can't relax to zero, while in chaotic and stochastic systems $C(\tau)$, does for large values of τ. This fact is in general interpreted as a "loss of memory" at some point the link between initial conditions and current state is completely forgotten by the system. When the quantity $C(\tau)$ is integrable one can find a characteristic "memory" time-scale τ_c for the system, as:

$$0 < \int_0^\infty d\tau C(\tau) = A < \infty \;\Rightarrow\; \tau_c = \frac{A}{C(0)} \tag{2.12}$$

Remark 2.2.5. Although chaos and stochasticity might appear the same for and external observer, the difference is deep, chaos is indeed deterministic while stochasticity is governed by distributions of probability.

2.3 Emergence and characterization of SC

2.3.1 Systems with special transients

- **Super-transients:** It has been shown via numerical simulations, that the dynamics of maps like (2.2) present a particularly long transient (called very imaginatively super-transient) followed by a stable phase characterized by motion along periodic orbits, as suggested by negativity of maximum LE.

  However,the length of the transient phase, scales exponentially with the dimension N of the system [5], thus if one considers, as pointed out before, the thermodynamical limit, Lyapunov stability is practically never reached. Phenomenon which makes clear the denomination "stable chaos".

  Remark 2.3.1. Convergence towards a periodic orbit implies the existence of a minimum threshold τ such that looking at the distance between two configurations $\{x_i\}_{i=1}^N(t)$, $\{x_i\}_{i=1}^N(t+\tau)$ for some $t > T$, this will tend to zero, which shows that τ is the period of the stable orbit and if T is the minimum possible time for this condition to be achieved, it will then be the transient length.

- **Unpredictable dynamics:** Another crucial aspect is that the dynamics is disordered and unpredictable for a wide range of coupling values as if it was generated by genuine chaotic CMLs [7, pag. 349].

  Indeed considering space and time correlation functions:

  $$C(j) = \frac{|\langle x_i(t)x_{i+j}(t)\rangle|}{x_i(t)^2} \quad C(\tau) = \frac{|\langle x_i(t)x_i(t+\tau)\rangle|}{x_i(t)^2}$$

  where $\langle\cdot\rangle$ is the ensemble average, one observes exponential decay [5].

  This is, as described before a clear sign of rather complex and unpredictable behavior in both space and time, testified by "loss of memory" at exponential rate.

2.3.2 ... and with special information propagation

Using the concept of comoving Lyapunov exponent revisited for finite sized perturbations we now examine the way perturbations propagate which strongly characterizes the phenomenon of stable chaos.

In DC the perturbation front evolves following linear mechanisms, the infinitesimal edge, which moves accordingly to $\Lambda(v_L) = 0$, pulls the core of the perturbation [9], forcing finite sized perturbation to evolve with the same velocity v_L. Moreover v_L is selected by the dynamics as the minimum allowed, in that, from (2.3) and the fact that $v_L = v_L(\mu^*)$ for some μ^* one finds:

$$\left.\frac{dv_L}{d\mu}\right|_{\mu=\mu^*} = \left.\frac{d}{d\mu}\left(\frac{\lambda(\mu)}{\mu}\right)\right|_{\mu=\mu^*} = \left.\frac{1}{\mu}\left(\frac{d\lambda}{d\mu} - \frac{\lambda}{\mu}\right)\right|_{\mu=\mu^*} = -\frac{\Lambda(v_L(\mu^*))}{(\mu^*)^2} = 0 \quad (2.13)$$

with

$$v_L = \frac{\lambda(\mu^*)}{\mu^*} = -\left.\frac{\lambda(\mu)}{d\mu}\right|_{\mu=\mu^*} \quad (2.14)$$

which shows that μ^* is a critical point and is a minimum being $\lambda(\mu)$ a Legendre transform (convex).

In SC non-linear mechanisms induce a faster propagation of information at speed $v_F \geq v_L$, it is like in front propagation discussed later where the front propagation is due to the pushing on the already saturated part towards the leading edge. Now comoving Lyapunov analysis allows one to take into account only for linear propagation mechanisms hence SC could be studied via numerical methods, only.

To better study the difference between those two phenomenon the parameter η has been introduced in (2.2). SC was, in fact, known to exist in discontinuous maps only i.e. for $\eta = 0$, introducing this parameter one could then have a continuous map, whose steepness could be controlled, the lower η the steeper the map (a condition whose effect turned out to be similar to that discontinuities), this idea lead to observation of SC also in continuous maps [5]. Moreover continuously varying the parameter, one could observe the transition from SC to DC together with some other interesting phenomena:

- **Entropy jumps:** While for $\eta = 0$ the topological entropy is null for $\eta \to 0^+$ there is a finite jump to $H_{topol} = \ln((1+\sqrt{5})/2)$, thus in principle genuine DC should be displayed.
- **Negative average Lyapunov exponent:** The average maximal Lyapunov exponent however changes continuously in η and after a threshold μ^* pass from being negative to positive, shifting from a Lyapunov stable system (SC indeed) to a genuine chaotic one.

Thus what happens is that for a little range $0 \leq \eta < \eta^*$ one has finite entropy with negative Lyapunov exponents.

Remark 2.3.2. Despite the average maximum LE being negative if one calculates LEs given by different initial conditions over a time span t, and then fabricates a probability $P(\lambda_{MAX}, t)$ out of the different results, (multi-fractal analysis), this would show the existence of a time increasing probability to have positive LEs. Figure 2.7 shows how despite being the average Lyapunov exponent still negative and increasing probability mass is moving towards the positive region.

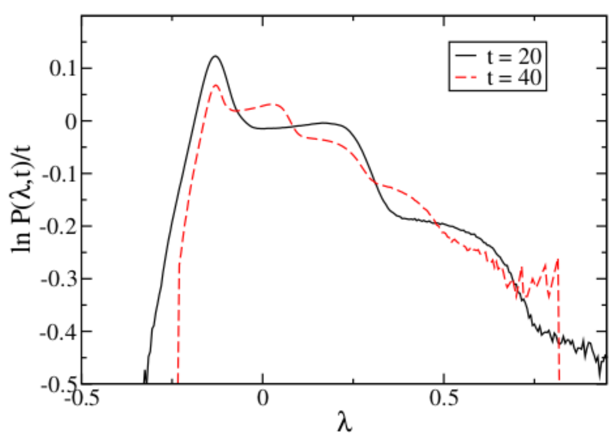

Figure 2.7: Multifractal distribution of Lyapunov exponents for $\eta = 1 \times 10^{-4}$, where the average Lyapunov exponent is still negative. This figure is taken from [5].

In order to better understand the action of non-linear mechanisms a finite perturbation propagation in coupled systems, comoving finite size Lyapunov exponents have been introduced [8], which are a generalization for CML of

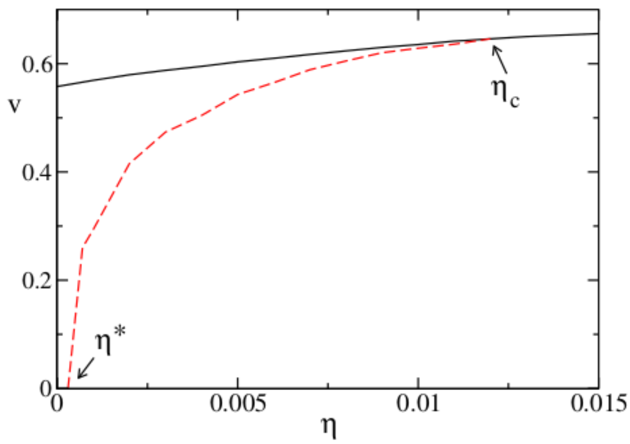

Figure 2.8: Linear velocity v_L (solid curve) and front velocity v_F (dashed curve) versus η. Deterministic chaos exists only for $\eta > \eta^*$. Beyond η_c, v_L and v_F coincide numerically. This figure is taken from [5].

FSLE. In Particular an analogy with formula $\Lambda(v_L) = 0$ has been conjectured and positively tested via numerical simulations:

$$\max_{\delta}\{\Lambda(\delta, v_F)\} = 0$$

The velocity of the front v_F is indeed higher of the linear one v_L discussed before, coming back to our system looking at Figure 2.8 one observes that for $\eta < \eta^*$ despite no linear velocity could be defined being the system stable (no propagation of infinitesimal perturbations is possible), the front is indeed propagating, moreover when η is sufficiently larger than η^*, v_F and v_L coincide numerically.

This shows that when $\lambda(\delta, 0) > \lambda(0, 0) = \lambda_{MAX}$, chaotic behaviour may be displayed also when dealing with "classically" stable systems, which is indeed the essence of SC.

2.4 Analogies with Reaction Diffusion Systems

We conclude this thesis trying to give physical relevance to the study of CMLs and stable chaos, in particular after an introduction to reaction-diffusion type of equation we will construct a parallel between perturbation evolution in CMLs and front propagations into unstable states in reaction-diffusion systems.

The perturbation evolution in spatially distributed systems can be described as the motion of an interface separating perturbed from unperturbed regions. In this spirit, one can wonder if and to what extent it is possible to draw an analogy between the evolution of this kind of interface and the propagation of fronts connecting steady states in reaction diffusion systems. Let us start by recalling the basic features of fronts propagation in reaction diffusion systems with reference to the Fisher-Kolmogorov-Petrovsky-Piscounov, FKPP equation:

$$\frac{\partial u(x,t)}{\partial t} = D\frac{\partial^2 u(x,t)}{\partial x^2} + f(u) \tag{2.15}$$

where $u(x,t)$ represents the concentration of a diffusing-reacting chemical specie and the chemical kinetics is governed by $f(u)$. Typically the function $f(u) \in C^1[0,1]$ with $f(0) = 0$, $f(1) = 0$, $f'(0) > 0$ $f'(1) < 0$. One immediately observes that this PDE exhibits one linearly stable $u = 1$ and one linearly unstable $u = 0$ stationary solution, since linearizing in time $f(u) = f'(0)u$ one sees that f drives small u away from zero. Once the system is prepared on the stable state $u(x) = 0 \; \forall \; x \in [0,1]$, an initial sufficiently steep perturbation, e.g. a delta function, will give rise to a smooth front with velocity $v^\dagger$, since this equation admits translating front solutions we could regard the front profile as an heteroclinic orbit in phase space connecting the unstable and the stable states, depending on the non-linearity $f(u)$ either pulled or pushed fronts will show up.

2.4.1 Front propagation into Unstable States: Linear Spread

If we take the spatial Fourier transform of our field $u(x,t)$:

$$\tilde{u}(k,t) = \int_{-\infty}^{+\infty} dx\, u(x,t)e^{-ikx}$$

Substitute the separation Ansatz : $\tilde{u}(k,t) = \tilde{u}(k)e^{-i\omega(k)t}$ Then we are given the dispersion relation $\omega(k)$, substituting the Fourier mode $^{ikx-i\omega(k)t}$ in the linearized FKPP equation around the unstable state yields:

$$\frac{\partial u(x,t)}{\partial t} = D\frac{\partial^2 u(x,t)}{\partial x^2} + f'(0)u(x,t) \tag{2.16}$$

$$\omega(k) = i(f'(0) - Dk^2)$$

Then $u = 0$ is linearly unstable if $\mathrm{Im}[\,\omega(k) > 0\,] = f'(0) - Dk_r^2 + Dk_i^2$, for some range of $k = k_r + ik_i$ values.

We then look at the linear spreading velocity:

$$v^* = \lim_{t\to\infty} \frac{dx_c(t)}{dt} \text{ with } u(x_C,t) = C \,\forall\, t$$

Which is well defined since being the evolution linear is independent of the chosen C.

Now given $\omega(k)$ and $\tilde{u}(k, t = 0)$ (which according to the ansatz is just the Fourier transform of the initial condition) one could determine the time evolution via inverse transform:

$$u(x,t) = \frac{1}{2\pi}\int_{-\infty}^{+\infty} dk\,\tilde{u}(k)e^{ikx-i\omega(k)t}$$

In order to determine the asymptotic speed v^* we first choose a co-moving frame $\xi = x - v^*t$ and write the transform in this new frame then applying the saddle point approximation for large t at the point K^* of the complex $k-$plane, in such a way that the time dependent part of the exponent varies the least, one has:

$$u(\xi,t) = \frac{1}{2\pi}\int_{-\infty}^{+\infty} dk\,\tilde{u}(k)e^{ik\xi-i(x-v^*t)+ikx-i\omega(k)t} = \frac{1}{2\pi}\int_{-\infty}^{+\infty} dk\,\tilde{u}(k)e^{ik\xi-i[\omega(k)-v^*k]t}$$

Pick k^* given by:

$$\left.\frac{d(\omega(k)-v^*k)}{dk}\right|_{k=k^*} = 0$$

Then in the ξ frame the perturbation neither increases nor decreases by definition of v^*, thus:

$$\omega_i - v^*k_i = 0 \Rightarrow v^* = \frac{\omega_i(k^*)}{k_i^*}$$

Where the indexes i, r stand for imaginary and real parts respectively. Finally set:

$$\lambda = k_i \text{ and } D = \mathrm{Re}\left[\left.\frac{i}{2}\frac{d^2\omega(k)}{dk^2}\right|_{k=k^*}\right]$$

to be the spatial decay rate of the perturbation, and the effective diffusion coefficient, in fact making use of the saddle point approximation and after a Gaussian integral one can show:

$$|u(\xi,t)| \sim \frac{1}{\sqrt{t}}e^{-\lambda^*\xi}e^{-\xi^2/4Dt}$$

For the linearized FKPP equation one has:

$$\mathrm{Re}\left[\left.\frac{i}{2}\frac{d^2\omega(k)}{dk^2}\right|_{k=k^*}\right] = D \text{ and } v^* = 2\sqrt{Df'(0)}$$

An important thing to note here is that the method adopted above made a crucial assumption, which is $\tilde{u}(k)$ being an entire function i.e. having no poles and therefore the growth of the integral being given by the exponential time dependent part, since as already noticed $\tilde{u}(k)$ given the ansatz is the Fourier transform of the initial condition. For this to be true we then must consider only steep enough initial condition like delta functions, or functions with compact support, it can be shown [17] that the condition:

$$\lim_{x\to\infty} u(x,t=0)e^{\lambda^*x} = 0$$

suffices.

2.4.2 Front propagation into Unstable States: Non-Linear Contributions

Let $v_{front}(t)$ be some suitably defined instantaneous front velocity. The crucial insight is that for front propagation, there are only two possibilities if we start from steep initial conditions:

- $\lim_{t\to\infty} v_{front}(t) = v^*$.
- $\lim_{t\to\infty} v_{front}(t) = v^\dagger > v^*$.

Where here we are assuming (not being particularly rigorous) that non-linearities can't kill the linear behaviour of the system, i.e that the dynamic is "local" and the only contribution of non-linear fronts is to speed up the linear velocity which is the one asymptotically chosen by the dynamics for steep enough initial conditions.

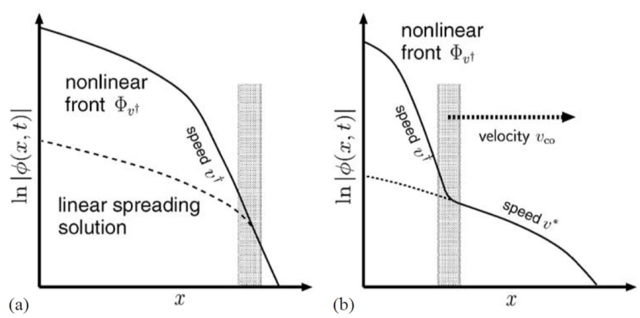

Figure 2.9: Illustration of the fact that when a non-linear front solution $\Phi_{v^\dagger}$ exists, whose asymptotic steepness is larger than λ^*, then this front will generically emerge: it is the selected pushed front solution. (a) shows that if the equation would be fully linear, the steep tail on the right, which moves at velocity larger than v^*, would cross over in the dashed region to the dashed profile moving with asymptotic speed v^*. However, this does not happen. When the steep profile matches up arbitrarily well with a fully non-linear profile,$\Phi_{v^\dagger}$, this faster front emerges. While (a) shows how only the pushed front solution ,$\Phi_{v^\dagger}$ can asymptotically emerge, (b) illustrates how a pushed front solution invades a region where the profile is close to that given by the linear spreading analysis. The dashed line indicates the profile obtained only via linear spreading analysis. This figure is taken from [17].

This is why one calls the first case pulled front, in which the linearities lead the dynamic while the second case takes then name of pushed front meaning that a crossover at some finite time of the non-linear front over the linear one takes place, governing thereon the asymptotic behaviour of the system.

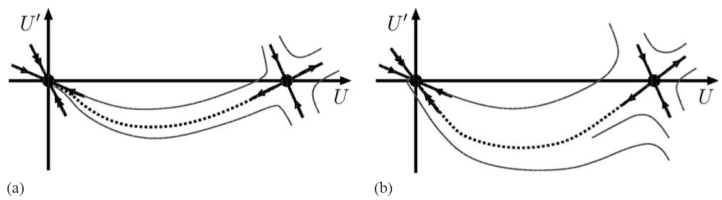

Figure 2.10: Sketch of the flow in the phase space $(U; U')$ shown are uniformly translating solutions. The solid lines at the two fixed points indicate the shape of the stable and unstable manifolds obtained by linearization. The arrows indicate the directions of the flow, and the double arrow at $(0; 0)$ indicates that the contraction along this eigendirection is stronger than along the other one $(\lambda_2 \geq \lambda_1)$. The dashed trajectory is the heteroclinic orbit connecting the two fixed points which corresponds to the front solution connecting the stable and the unstable state. (a) shows the case $v = max(v^\dagger; v^*)$, in fact the trajectory approaches the origin along the slowest contracting direction. (b) instead displays what happens if for some $v = v^\dagger$ the dashed trajectory becomes a "strongly heteroclinic orbit" which approaches the origin along the strongly contracting direction i.e. the equation admits a pushed front solution. This figure is taken from [17].

For the FKPP one could go deeper and observe that admits a family of uniformly translating solutions, parametrized by v, namely:

$$u(x, t) = U_v(\xi) = U_v(x - vt)$$

We could then build a coupled system of differential equations, in this new frame:

$$\frac{dU(\xi)}{d\xi} = U'$$

$$\frac{dU'(\xi)}{d\xi} = -\frac{v}{D}U'(\xi) - \frac{1}{D}f(U)$$

Looking at stability matrices at $(0, 0)$ and $(0, 1)$, in the frame (U, U') one sees that the origin is a stable fixed point while $(0, 1)$ is unstable, in this sense one could regard the translating front as an heteroclinc orbit connecting those 2 fixed points. Given the dimensionality of the system we distinguish 2 cases:

- The orbit asymptotically reaches the slowest contracting direction, which we will see corresponds to pulled fronts.
- The orbit asymptotically reaches the strongest contracting direction, which instead corresponds to pushed fronts.

Our solution in the neighbourhood of the origin and for some admissible $v^\dagger \geq v^*$ (whose existence is proved in [18]) will look like:

$$U_{v^\dagger}(\xi) \approx a_1 e^{-\lambda_1 \xi} + a_2 e^{-\lambda_2 \xi}$$

Where a_1,a_2 can be found only considering the full non-linear behaviour, and λ_1, λ_2 are the linear decaying rates along the two orthogonal contracting directions given by the stability matrix at the origin.

Thus condition $a_1 = 0$ is sufficient to observe a pushed front since any linear character we have seen would fall as $e^{-\lambda^* \xi}$ for large ξ leaving space for faster $v^\dagger \geq v^*$ and steeper non-linearities to prevail [17].

We could give an approximation for the maximum speed achievable by a uniformly translating solution calculating the dispersion relation and the spreading velocity v^*_{max} considering the bound from above of $f(u)$ given via:

$$f(u) \leq \sup_{0 \leq u \leq 1} \left[\frac{f(u)}{u} \right] u$$

Which gives a linear spreading:

$$v^*_{max} = 2\sqrt{D \sup_{0 \leq u \leq 1} \left[\frac{f(u)}{u} \right]}$$

If then the criterium above, which depends on the functional form of $f(u)$, allows for a pushed front the admissible velocities will lie in $[v^*, v^*_{max}]$ (a more rigorous geometrical argument in favour of those bounds is given in [18]).

2.4.3 CMLs and Reaction-Diffusion Systems

We know move to the comparison between the CML illustrated above and the FKPP equation.

We start with a direct comparison between 2.12 and the shapes for the fronts sketched in Figure 2.9, it is immediate to note ,how despite being rather different systems the behaviour is surprisingly similar.

What we want to analyse is the spreading of perturbations in a chaotic system. In order to compare our case with the FKPP, we should consider the time evolution of the difference of two (initially nearby) chaotic trajectories $\{\delta x_i\}_{i=1}^{L}$. However, the nature of the two phases separated by the front is now different from the FKPP case. The interface separates in fact an unstable ($\delta x_i = 0$ because of SIC) state from a fluctuating one (chaotic) in the bulk of the perturbation, which is clearly not stable in a usual sense. However taking a statistical mechanic approach one could observe that it fluctuates in a stationary way around an average value, so we might say is " statistically stable " and therefore by averaging the perturbation evolution over many different initial conditions, many similarities could be observed. Once the chaotic fluctuations are neglected, one can express the average perturbation growth in any site of the chain via the following mean-field approximation:

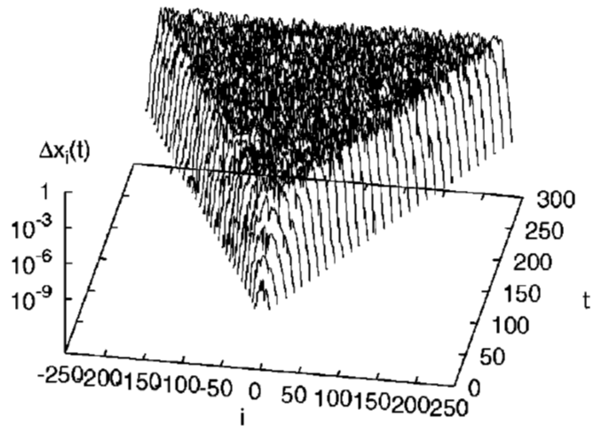

Figure 2.11: Evolution of the perturbation $\Delta x_i(t)$, for a chain of coupled tent map lattices with a coupling $\epsilon = 2/3$. The initial perturbation is taken as 10^{-8}. This is an example of pulled front. This figure is taken from [9].

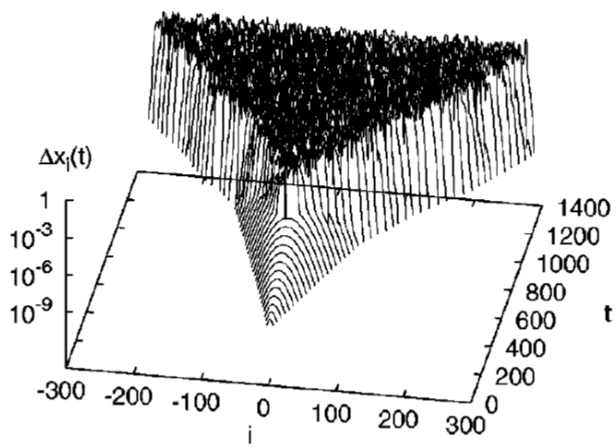

Figure 2.12: Evolution of the perturbation $\Delta x_i(t)$, for a chain of coupled shift map lattices with a coupling $\epsilon = 1/3$ and parameter $\beta = 1.03$. The initial perturbation is taken as 10^{-8}. This is an example of pushed front, in that after an initial stage similar to Fig. 2.6 an higher velocity is selected. This figure is taken from [9].

$$u_i(t+1) = e^{\lambda(\tilde{u}_i(t))}\tilde{u}_i(t)$$

with:

$$\tilde{u}_i(t) = (1-\epsilon)u_i(t) + \frac{\epsilon}{2}\Big[u_{i-1}(t) + u_{i+1}(t)\Big]$$

Reorganize the equation as follows:

$$u_i(t+1) = e^{\lambda(\tilde{u}_i(t))}\Big[(1-\epsilon)u_i(t) + \frac{\epsilon}{2}[u_{i-1}(t) + u_{i+1}(t)]\Big]$$

Introduce discrete time and space resolutions δt and δx related by diffusive scaling $\delta t \sim \delta^2 x$:

$$\frac{u_i(t+\delta t) - e^{\lambda(\tilde{u}_i(t))\delta t}u_i(t)}{\delta t} = e^{\lambda(\tilde{u}_i(t))\delta^2 x}\frac{\epsilon}{2}\frac{[(u_{i-\delta x}(t) + u_{i+\delta x}(t) - 2u_i(t)]}{\delta^2 x}$$

Expand, order zero in space and first order in time the exponential for small δ's :

$$\frac{u_i(t+1) - (1-\lambda\delta t)u_i(t)}{\delta t} = \frac{\epsilon}{2}\frac{[u_{i-1}(t) + u_{i+1}(t) - 2u_i(t)]}{\delta^2 x}$$

Finally taking the limit $\delta t, \delta^2 x \to 0$:

$$\partial_t u(x,t) - \lambda(u)u = \frac{\epsilon}{2}\partial_{xx}u(x,t)$$

If we set $D = \epsilon/2$ and $f(u) = \lambda(u)u$ one recovers the FKPP equation, moreover:

$$v^* = \sqrt{2\epsilon\lambda}$$
$$v^*_{max} = \sqrt{2\epsilon \sup_{0\le u\le 1}\lambda(u)}$$

It is interesting to note how the model obtained from the FKPP matches numerical prediction of V_p using the marginal stability criterium described before with comoving FSLE, comoving LE and direct measurement.

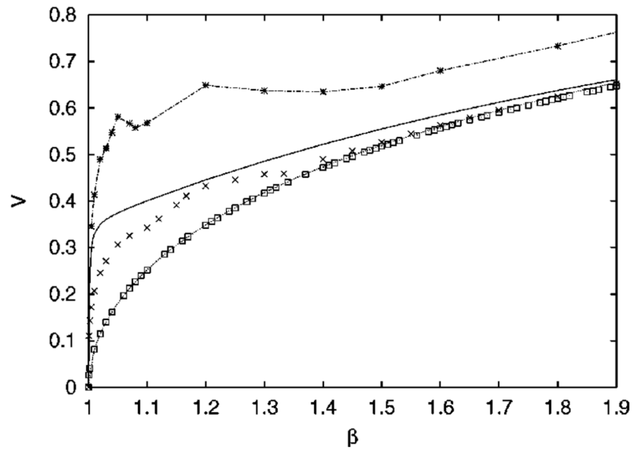

Figure 2.13: Information propagation velocities for the shift map with $\beta = 1/3$: boxes=linear velocities V_L and crosses=directly measured nonlinear ones. The two lines correspond to v^*=dotted line and to the propagation velocity for the comparison model with $\lambda(u)$ given by $\sqrt{2\epsilon \max_u\{\lambda(u)/u\}}$=solid line. The dashed curve with asterisks is $\sqrt{2\epsilon \max_\delta\{\lambda(\delta)\}}$.

Conclusions

What this work has definitely pointed out is the variety of techniques that could be used in analysing a problem in the field of dynamical systems. What really struck me initially, and what I feel it is really the gap between mathematics and applications, is the fact that in order to introduce rigour one has to give definitions and most of these are set in order to prove a particular result. Here I am not saying that one loses generality but rather that different approaches to the same problem may lead to a different contextualisation of the subject making it sometimes difficult to understand the real property one wants to point out when imposing some mathematical structure. A clear example of this is the definition of SIC in a topological sense or in the Lyapunov exponent sense, seen in the first paragraphs. However, I find this really intriguing. It is indeed, a clear signal of how the field is vast and from how many radically different points of view one could look at it, topology and geometry, ergodic theory, functional analysis and sometimes even number theory finds its place, this just to mention the more abstract parts. There is in fact, also a strong computational aspect, which is not really treated in this work but surrounds each result and statement, in the sense that the main source of information here is indeed given by numerical simulations from which, strictly mathematical objects, like theorems and propositions may later rise. Despite my original idea of writing a more standard mathematical work, it turned out that for some parts was not even possible to find a well-established formal theory and this leaves open space for research and new possible studies. This paper shows that no mathematical theory of stable chaos exists but only facts emerging from numerical simulations. Exploring general conditions behind the existence of such a phenomenon could actually be a possible topic of research for the future.

Bibliography

[1] Robert Devaney, *"An introduction to chaotic dynamical systems"*, Addison-Wesley, pag. 50, 1989

[2] Michel Brin and Garrett Stuck, pag. 24 and 82, 1998. *"Introduction to Dynamical Systems"*, Cambridge University Press.

[3] D. Ruelle *"What is a strange attractor?"*, Notices of AMS, August, 2006, Volume 53, Issue 7.

[4] D. Ruelle *"Les attracteurs étranges"*, La Recherche, nr. 108, 1980

[5] Antonio Politi and Alessandro Torcini, *"Stable Chaos"*, arXiv:0902.2545 [nlin.CD], 2009

[6] D. Ruelle, *"Large volume limit of the distribution of characteristic Lyapunov exponents in turbolence"*, pag. 287

[7] Angelo Vulpiani, Massimo Cencini, Fabio Cecconi, *"Chaos: From Simple Models to Complex Systems"*, World Scientific.

[8] Massimo Cencini, Alessandro Torcini, *"Linear and Nonlinear information flow in spatially extended systems"*, Phys. Rev. 2001.

[9] Grassberger P., Politi A., Torcini A., *"Error propagation in extended chaotic systems"*, Journal of Physics A: Mathematical and General, Volume 28, Number 16.

[10] Robert May, *"Simple mathematical models with very complicated dynamics"*, Nature 261, 1976.

[11] Livi R.,Politi A.,Oppo G.,Kapral R., *"Unpredicatable behavior of stable systems"*, Europhys. Lett. 22, pag. 571-576, 1993.

[12] Eli Glasner, Benjamin Weiss, *"Sensitive dependence on initial conditions"*, Nonlinearity 6, pag. 1067–1075, 1993.

[13] Edward Ott, *"Chaos in dynamical systems"*, Cambridge University Press, 1993.

[14] D. Ruelle, *"Ergodic theory of differentiable dynamical systems"*, Publ. Math. 1979.

[15] Lai-Sang Young, *"Mathematical theory of Lyapunov exponents"*, J. Phys. A: Math. Theor. 46, 2013.

[16] David Angulo-Garcia, Alessandro Torcini, *"Stable chaos in fluctuation driven neural circuits"*, arXiv:1403.0464 [cond-mat.dis-nn],2014.

[17] Wim van Saarloos, *"Front propagation into unstable states"*, Physics Reports 386, pag. 29–222, 2003.

[18] D. G. Aronson, H. F. Weinberger, *"Non linear diffusion in population genetics, combustions, nerve pulse propagation"*, Adv. Math. 30, 33, 1978.

[19] Lorenz, Edward Norton. *"Deterministic nonperiodic flow"*. Journal of the Atmospheric Sciences 20, pag.130–141, 1963.

[20] Yakov Pesin, Dr. Boris Hasselblatt. *"Nonuniform hyperbolicity"*. Scholarpedia, 3(1):4842, 2008.

[21] L.A. Bunimovich, Ya.G. Sinai, *"Spacetime chaos in coupled map lattices"*, Nonlinearity 1 (4), pag.491-516, 1988.

[22] Aurelien Kenfack Jiotsa, Antonio Politi, Alessandro Torcini *"Convective Lyapunov spectra"* J. Phys. A: Math. Theor. 46, 2013

[23] G. Benettin, L. Galgani, A. Giorgilli and J.M. Strelcyn, *"Lyapunov characteristic exponents for smooth dynamical systems and for Hamiltonian systems; a method for computing all of them, part 1:theory"*, Meccanica, 15, pag. 9–20, 1980.

[24] Suneel Madhekar's blog on chaos and non-linear phenomena. hyperchaos.wordpress.com